MICHIGAN STATE UNIVERSITY

CYCLOTRON PROJECT*

Run 26 Field Information

H. G. Blosser and D. A. Flanigan

October 1960

Department of Physics

East Lansing, Michigan

*Research supported in part by the U. S. Atomic Energy Commission
Contract Numbers AT(40-1)-2425 and AT(11-1)-872.

Run 26 Field Information

In the summer of 1958 field measurements for a number of cyclotron magnet configurations were made by the magnet group[1] of the Oak Ridge National Laboratory with whom the authors were working in collaboration at the time. One of these field surveys known as Run 26 has since been employed as the basic field configuration in an extensive series of orbit studies at Michigan State; the results of these orbit studies are the subject of reports and papers in press or in preparation. In view of extensive interpretations inferred from Run 26 orbit studies it is deemed worthwhile to herein set forth the original field data to serve as reference and background for interpretive reports.

The model magnet configuration for Run 26 embodies a three sector pole tip of design due to one of the authors (HGB) operated at a magnetic field of roughly 14 kilogauss averaged over hills and valleys. Page 3 of this report is a sketch of the magnet configuration. Pages 4 and 5 give the direct magnetic data in terms of divisions on a strip chart potentiometer used for recording the data. The data points are a square grid (1/4" x 1/4" squares) covering 1/2 of the magnet pole. Page 6 is a hand drawn contour map made from the measured data (the field in the unmeasured half of the magnet is inferred by assuming 120° symmetry). Page 7 is a graph of field versus azimuth at a number of radii;

---

1. Cohen, Blosser, Hudson, Lord, and Bender, Nuclear Instruments 6, 105 (1960)

a decided squarishness of the waveform and considerable broadening of the hill regions both are quite evident at larger radii.

Results of Fourier analysis of the field data are presented on pages 8, 9, and 10. To accomplish the analysis field values on a polar mesh were inferred by 16 point (4 x 4) two dimensional interpolation in the rectangular field grid. The azimuthal spacing in the polar mesh was 3.75°, the radial spacing 0.1". The respective B_i, H_i, G_i, and δ_i were determined by numerical integration as implied by the respective field formulae given on pages 8 and 10. The amplitudes of the respective Fourier components are plotted vs. radius on page 11; the respective spiral angle for each is given on page 12. In the computation of the H_i, G_i, etc. $\theta = 0$ is taken in the direction shown on page 3 and the 120° section of field data from $\theta = 30^{\circ}$ to $\theta = 150^{\circ}$ was employed for the computation.

It is a pleasure to acknowledge our indebtedness to the Oak Ridge National Laboratory and especially to E. D. Hudson, R. S. Livingston, and R. S. Lord for making available to us the facilities and data from which the results of this report are derived.

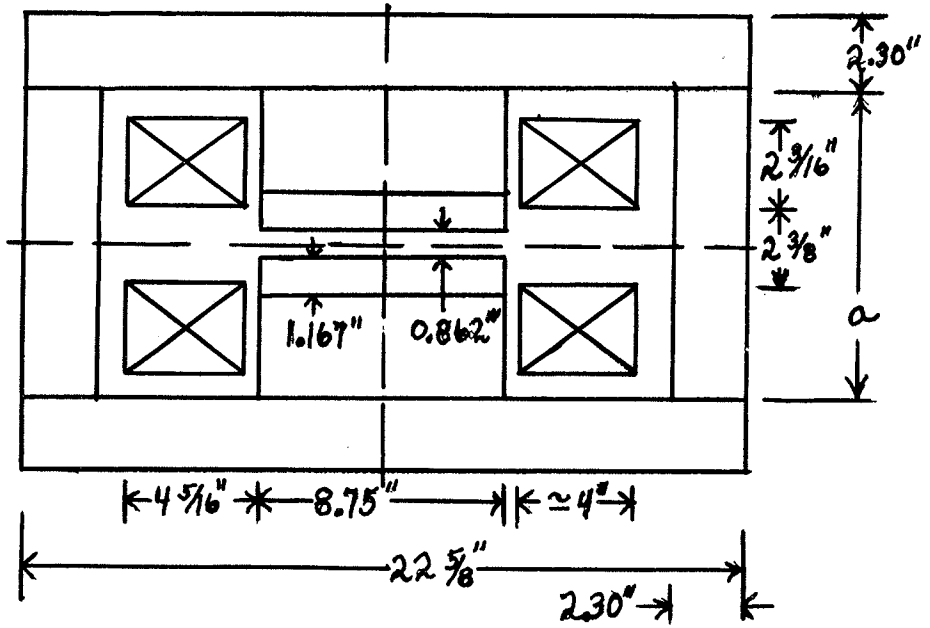

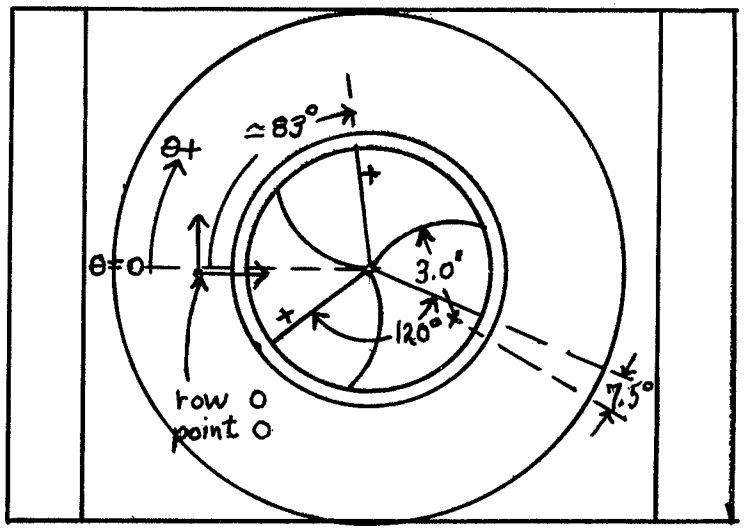

View of Upper Pole

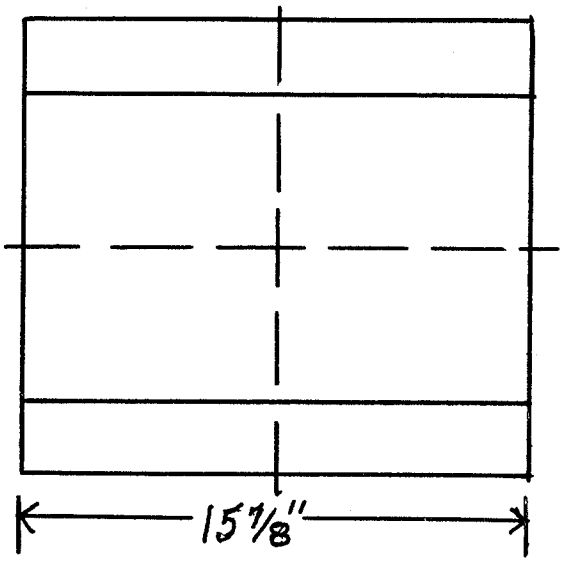

RUN 26 MAGNET SET UP

Magnet - 1010 steel. Coils - copper. 240 turns total (120 each coil) 253.3 amps/turn - 60.8×10^3 amp-turns
Recording chart: B = 0 corresponds to 5.7 divisions below zero on chart. 1 chart division = 225.7 gauss. With respect to sketch at left measurements cover upper half of pole beginning at row 0 point 0 mark. Measurements made 6-30-58

row # / point #	0	1	2	3	4	5	6	7	8	9	10
0	15.3	15.4	15.2	15.0	14.3	13.5	12.7	11.8			
1	20.5	20.6	20.1	19.7	18.9	17.7	16.5	15.2	14.0	12.7	
2	28.2	28.2	27.7	26.7	25.4	23.6	21.8	19.9	18.0	16.0	14.2
3	39.9	39.9	39.1	37.7	35.6	32.7	29.7	26.7	23.6	20.7	18.1
4	54.7	54.7	53.7	52.0	49.4	45.7	41.4	36.7	31.9	27.4	23.3
5	65.3	65.1	64.5	63.4	61.7	58.7	54.8	49.8	43.4	36.9	30.8
6	70.0	69.9	69.4	69.0	67.9	66.1	63.7	60.1	55.2	48.4	40.7
7	71.9	71.8	71.5	71.1	70.4	69.1	67.5	65.1	62.0	57.3	50.7
8	72.9	72.7	72.6	72.2	71.3	70.2	68.7	66.9	64.2	60.6	55.8
9	73.2	73.2	73.0	72.5	71.7	70.4	68.7	66.4	63.2	59.6	55.1
10	73.4	73.5	73.2	72.5	71.7	69.4	66.3	62.6	57.8	53.2	48.3
11	73.7	73.6	73.2	71.9	69.8	65.6	60.1	54.2	48.4	43.8	39.9
12	73.8	73.5	72.4	69.7	65.0	58.0	50.8	44.8	40.2	37.0	34.4
13	73.6	72.6	70.0	65.0	57.2	49.1	42.8	38.4	35.2	33.3	31.7
14	72.6	70.5	65.6	57.5	49.0	42.2	37.8	34.9	32.9	31.6	30.6
15	70.8	67.1	59.5	50.2	42.9	37.9	35.0	33.2	31.8	31.0	30.4
16	67.9	62.4	53.4	44.7	39.3	35.8	33.9	32.8	31.8	31.2	30.9
17	64.7	57.8	48.6	41.6	37.7	35.3	34.1	33.5	33.0	32.9	32.8
18	61.2	54.1	45.8	40.7	37.7	36.6	36.0	36.1	36.2	36.4	36.8
19	57.3	51.4	45.1	41.7	40.5	40.4	40.8	41.7	42.6	43.5	44.6
20	53.6	50.4	47.1	46.4	47.1	48.3	49.8	51.7	53.2	54.9	56.3
21	51.3	51.0	51.7	53.9	56.4	58.8	60.9	63.1	64.4	65.7	66.5
22	51.4	51.4	53.9	58.7	62.6	65.6	67.7	69.4	70.3	70.9	71.2
23	51.7	48.6	50.6	56.6	62.8	67.2	70.0	71.9	72.5	72.8	72.8
24	49.9	44.9	45.3	50.6	58.5	65.8	70.2	72.4	73.0	73.4	73.4
25	46.8	41.7	41.2	45.0	52.6	62.1	69.0	72.4	73.2	73.5	73.5
26	43.5	39.0	38.3	41.0	47.3	57.2	66.6	71.5	73.1	73.6	73.5
27	40.5	36.8	36.2	38.2	43.3	52.6	63.4	70.1	72.7	73.6	73.5
28	38.1	35.2	34.6	36.2	40.5	48.8	60.1	68.7	72.0	73.2	73.2
29	36.0	33.8	33.5	34.8	38.6	45.9	57.1	66.9	71.2	72.7	73.0
30	34.5	32.7	32.5	33.8	37.2	43.9	54.6	65.1	70.1	71.8	72.4
31	33.1	31.7	31.8	33.1	36.2	42.5	52.8	63.6	69.0	70.9	71.4
32	31.9	31.0	31.0	32.4	35.6	41.6	51.8	62.4	67.8	69.8	70.1
33	30.8	30.2	30.6	32.0	35.2	41.3	51.6	61.6	66.4	68.3	68.4
34	29.9	29.5	30.0	31.4	35.0	41.4	51.6	60.8	64.9	66.1	65.7
35	28.7	28.7	29.3	31.0	34.9	41.8	51.6	59.4	62.4	62.6	60.5
36	27.5	27.5	28.4	30.3	34.5	41.9	51.0	56.7	57.8	55.9	51.1
37	25.9	26.0	27.1	29.1	33.5	40.8	47.8	50.7	49.2	45.0	39.2
38	24.1	24.2	25.2	27.0	30.8	36.4	40.2	40.2	37.3	33.4	29.2
39	21.9	22.1	22.8	24.0	26.3	29.1	30.3	29.5	27.3	24.7	22.0
40	19.6	19.6	20.1	20.7	21.7	22.5	22.7	22.0	20.5	18.9	17.2
41	17.0	17.1	17.4	17.6	17.8	17.9	17.7	17.1	16.0	14.9	13.7
42	14.5	14.6	14.7	14.7	14.7	14.5	14.2	13.6	12.7	11.8	
43	12.2	12.2	12.3	12.1	12.0	11.8	11.3	10.9			

Run 26 Field Data. Rows and points uninformily spaced on square grid of mesh 1/4" x 1/4". Field is given as divisions on recorder chart. Magnet center is half way between points 21 and 22 and rows 0 and 1.

row #	11	12	13	14	15	16	17	18	19	20	21
point #											
0											
1											
2	12.7										
3	15.9	13.8	11.9								
4	20.1	17.1	14.4	12.5							
5	25.6	21.3	17.6	15.0	12.8						
6	33.3	26.7	21.5	17.8	14.9	12.2					
7	42.3	33.7	26.2	20.9	17.1	14.0	11.6				
8	49.1	40.2	30.9	24.1	19.3	15.7	12.9	10.9			
9	49.7	42.3	33.4	26.1	21.0	17.2	14.4	12.2	10.3		
10	43.5	38.2	32.0	26.3	22.0	18.5	15.7	13.4	11.4		
11	36.4	33.2	29.2	25.8	22.6	19.4	16.9	14.6	12.6	10.6	
12	32.3	30.2	27.7	25.5	23.1	20.4	18.0	15.8	13.7	11.6	
13	30.3	29.1	27.2	25.7	23.8	21.5	19.2	16.9	14.8	12.6	10.6
14	29.7	28.8	27.3	26.3	24.8	22.7	20.4	18.3	15.9	13.6	11.5
15	29.8	29.1	28.2	27.3	26.1	24.1	22.0	19.8	17.2	14.7	12.3
16	30.8	30.3	29.7	29.1	28.0	26.2	24.1	21.7	18.8	15.9	13.3
17	33.0	32.9	32.6	32.2	31.4	29.8	27.4	24.5	21.0	17.4	14.3
18	37.6	37.9	37.8	38.1	37.7	36.2	33.6	29.3	24.0	19.2	15.6
19	45.9	46.9	47.4	48.0	48.0	46.6	43.1	36.3	27.9	21.2	16.7
20	57.9	58.7	59.4	59.6	59.2	57.1	52.4	43.0	31.6	23.1	17.7
21	67.3	67.4	67.4	66.7	65.8	63.1	57.7	47.2	34.0	24.4	18.3
22	71.6	71.2	70.7	69.9	68.6	65.7	60.0	49.0	35.2	25.0	18.7
23	73.1	72.7	72.0	71.2	69.9	66.8	60.8	49.2	35.2	25.1	18.7
24	73.5	73.1	72.5	71.8	70.5	67.1	60.7	48.1	34.3	24.5	18.3
25	73.6	73.1	72.5	71.9	70.4	66.9	59.1	46.0	32.6	23.4	17.7
26	73.4	73.1	72.5	71.9	70.2	65.9	56.7	42.9	30.3	22.1	16.7
27	73.4	73.1	72.5	71.6	69.4	63.8	52.9	39.1	27.8	20.5	15.6
28	73.3	73.0	72.3	70.8	67.7	60.4	47.9	34.9	25.2	18.9	14.5
29	73.0	72.4	71.5	69.4	65.1	55.3	42.1	30.6	22.6	17.1	13.3
30	72.3	71.7	70.2	67.2	60.6	48.7	35.9	26.6	20.0	15.4	12.2
31	71.3	70.4	68.1	63.2	53.7	41.2	30.3	22.9	17.6	13.8	
32	69.7	68.2	64.4	56.7	45.3	33.9	25.4	19.8	15.4	12.2	
33	67.4	64.3	57.8	47.7	36.7	27.7	21.4	16.9	13.4		
34	63.0	57.2	48.2	37.9	29.3	22.7	17.9	14.6	11.7		
35	55.1	46.8	37.7	29.8	23.5	18.8	15.2	12.5			
36	43.8	35.9	29.1	23.4	19.0	15.6	12.8				
37	32.9	27.3	22.7	18.8	15.6	13.0					
38	24.9	21.1	18.2	15.3	12.8						
39	19.3	16.7	14.7	12.6							
40	15.3	13.5	12.0								
41	12.3										
42											
43											

Run 26 Field Data (cont.)

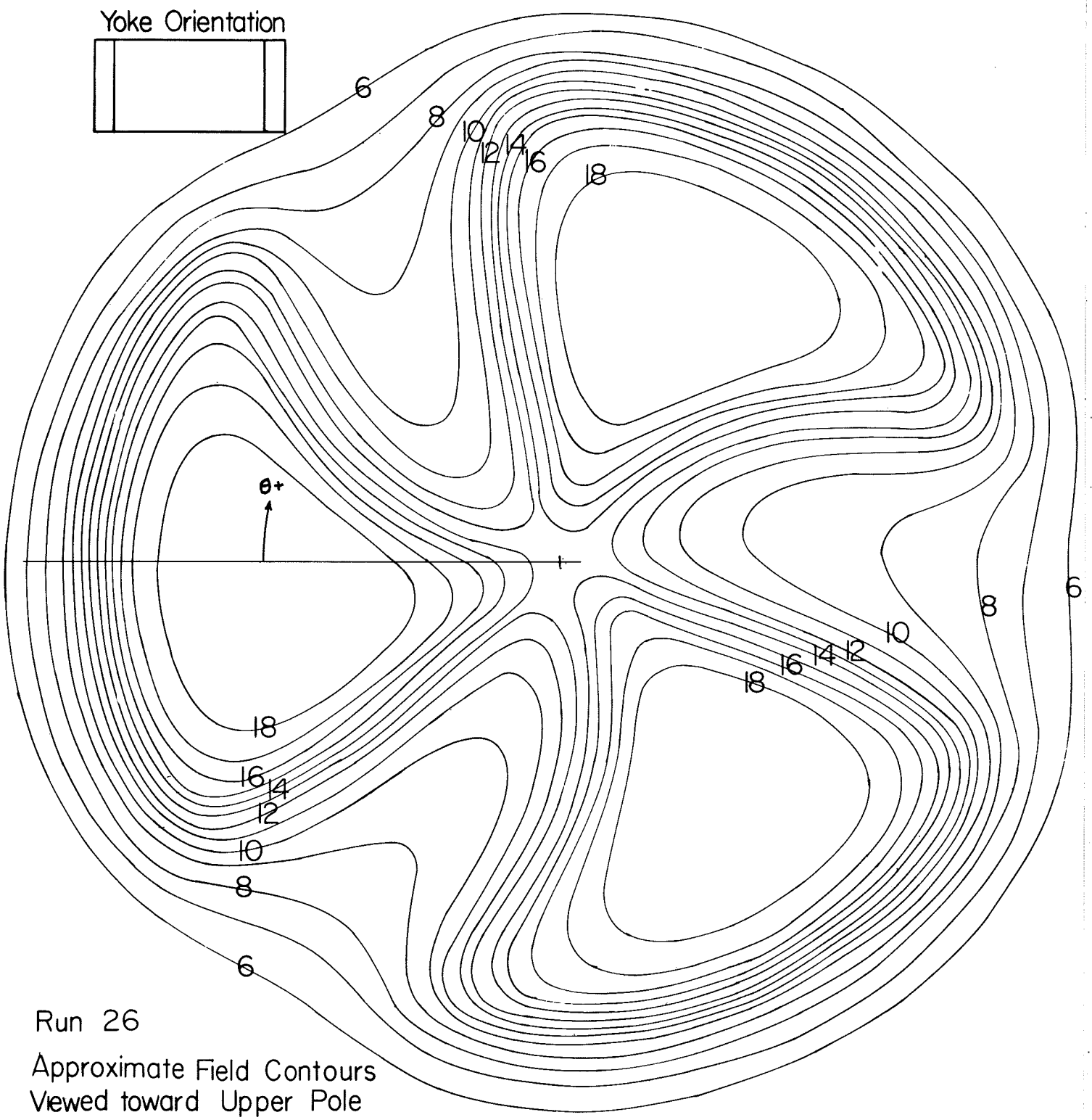

Run 26

Approximate Field Contours
Viewed toward Upper Pole
Field in Kilo-gauss

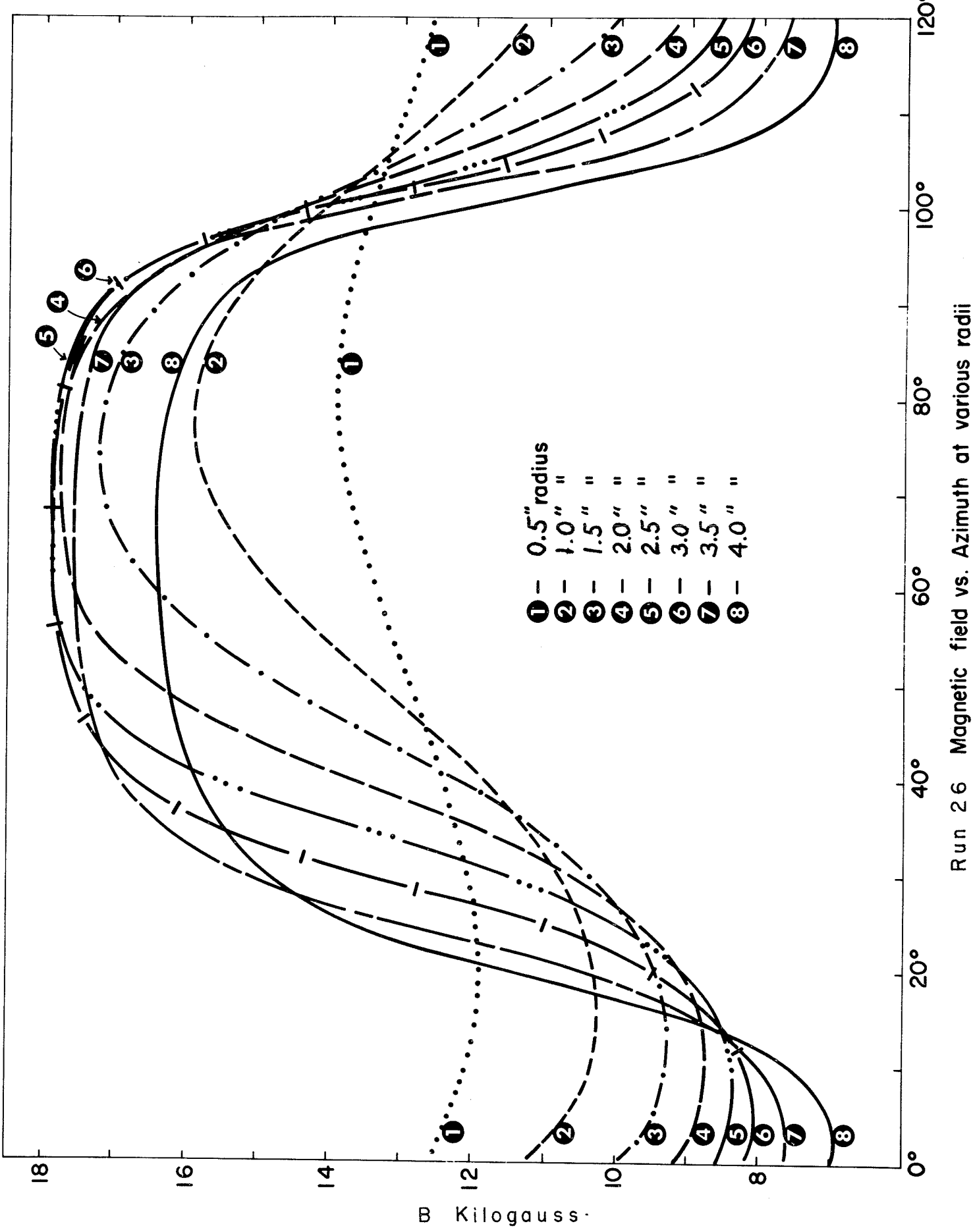

Run 26 Magnetic field vs. Azimuth at various radii

r inches model	B_o gauss	H_3 gauss	G_3 gauss	H_6 gauss	G_6 gauss	H_9 gauss	G_9 gauss
0.1	+12865	+00015	-00010	-00002	+00001	+00001	-00000
0.2	+12890	+00077	-00096	+00001	+00014	+00002	-00006
0.3	+12895	+00183	-00276	+00008	+00024	+00001	-00018
0.4	+12892	+00340	-00520	+00001	+00030	-00003	-00027
0.5	+12907	+00559	-00821	-00011	+00021	-00002	-00037
0.6	+12928	+00827	-01136	-00017	+00009	+00001	-00035
0.7	+12945	+01113	-01430	-00014	-00008	+00010	-00029
0.8	+12960	+01395	-01688	-00023	-00033	+00026	-00021
0.9	+12985	+01682	-01914	-00032	-00059	+00038	-00015
1.0	+13016	+01971	-02104	-00038	-00077	+00051	+00007
1.1	+13054	+02259	-02259	-00046	-00089	+00067	+00038
1.2	+13101	+02547	-02377	-00047	-00094	+00086	+00071
1.3	+13155	+02835	-02461	-00045	-00086	+00105	+00116
1.4	+13217	+03112	-02519	-00048	-00064	+00116	+00172
1.5	+13288	+03373	-02561	-00062	-00032	+00117	+00231
1.6	+13364	+03621	-02575	-00081	+00012	+00108	+00289
1.7	+13435	+03854	-02551	-00100	+00068	+00090	+00348
1.8	+13497	+04064	-02490	-00131	+00133	+00060	+00407
1.9	+13552	+04249	-02410	-00183	+00201	+00020	+00460
2.0	+13605	+04412	-02321	-00259	+00268	-00026	+00505
2.1	+13656	+04562	-02223	-00346	+00329	-00077	+00538
2.2	+13706	+04699	-02108	-00438	+00384	-00130	+00557
2.3	+13753	+04819	-01983	-00534	+00432	-00181	+00564
2.4	+13800	+04921	-01858	-00637	+00471	-00229	+00560
2.5	+13847	+05008	-01741	-00755	+00498	-00271	+00545
2.6	+13892	+05081	-01625	-00875	+00514	-00308	+00515
2.7	+13929	+05136	-01497	-00988	+00517	-00337	+00470
2.8	+13959	+05175	-01355	-01095	+00508	-00353	+00417
2.9	+13980	+05205	-01211	-01199	+00484	-00352	+00368
3.0	+13997	+05231	-01064	-01306	+00449	-00336	+00322
3.1	+14007	+05254	-00917	-01409	+00401	-00309	+00278
3.2	+14008	+05266	-00773	-01505	+00341	-00273	+00239
3.3	+14001	+05263	-00636	-01594	+00267	-00228	+00200
3.4	+13984	+05251	-00508	-01676	+00183	-00174	+00165
3.5	+13953	+05231	-00391	-01749	+00094	-00116	+00141
3.6	+13894	+05199	-00277	-01805	+00002	-00058	+00126
3.7	+13798	+05149	-00160	-01843	-00089	-00004	+00117
3.8	+13652	+05073	-00039	-01858	-00177	+00046	+00113
3.9	+13439	+04962	+00077	-01848	-00258	+00091	+00117
4.0	+13130	+04796	+00167	-01814	-00327	+00126	+00132
4.1	+12689	+04547	+00227	-01749	-00375	+00149	+00151
4.2	+12079	+04189	+00262	-01632	-00399	+00151	+00158
4.3	+11303	+03721	+00265	-01465	-00393	+00145	+00156
4.4	+10410	+03174	+00226	-01269	-00356	+00133	+00152
4.5	+09469	+02600	+00164	-01064	-00293	+00127	+00143
4.6	+08551	+02058	+00115	-00859	-00227	+00119	+00122
4.7	+07711	+01596	+00094	-00669	-00172	+00095	+00097
4.8	+06974	+01228	+00091	-00502	-00137	+00061	+00067

Fourier coefficients as functions of radius for Run 26 field

$$B(r,\theta) = B_o(r) + \sum_{j=1} \left(H_{3j}(r) \cos 3j\theta + G_{3j}(r) \sin 3j\theta \right).$$

r inches model	H_{12} gauss	G_{12} gauss	H_{15} gauss	G_{15} gauss	H_{18} gauss	G_{18} gauss
0.1	-00000	+00000	+00000	-00000	-00000	+00000
0.2	-00001	+00007	-00000	-00004	-00001	+00004
0.3	-00000	+00010	+00001	-00011	-00000	+00008
0.4	-00002	+00014	-00000	-00011	-00002	+00011
0.5	-00004	+00020	-00000	-00012	-00000	+00014
0.6	-00006	+00027	+00000	-00013	+00001	+00015
0.7	-00009	+00026	+00004	-00016	+00003	+00015
0.8	-00007	+00025	+00005	-00013	+00001	+00014
0.9	-00003	+00018	+00006	-00013	+00001	+00014
1.0	+00002	+00016	+00003	-00015	+00003	+00013
1.1	+00008	+00017	-00000	-00013	+00003	+00014
1.2	+00019	+00017	+00001	-00013	+00002	+00016
1.3	+00027	+00019	-00000	-00011	+00000	+00018
1.4	+00028	+00023	-00009	-00009	-00006	+00016
1.5	+00025	+00019	-00018	-00009	-00006	+00013
1.6	+00024	+00013	-00023	-00011	-00004	+00016
1.7	+00021	+00011	-00030	-00013	-00004	+00017
1.8	+00018	+00004	-00037	-00023	-00005	+00014
1.9	+00014	-00010	-00042	-00037	-00003	+00010
2.0	+00011	-00034	-00048	-00049	+00004	+00012
2.1	+00009	-00066	-00055	-00061	+00009	+00017
2.2	+00010	-00104	-00057	-00074	+00012	+00022
2.3	+00022	-00142	-00050	-00086	+00015	+00029
2.4	+00045	-00179	-00038	-00093	+00020	+00041
2.5	+00079	-00211	-00026	-00089	+00024	+00055
2.6	+00114	-00237	-00019	-00081	+00021	+00070
2.7	+00151	-00257	-00014	-00069	+00007	+00084
2.8	+00197	-00273	-00010	-00056	-00009	+00096
2.9	+00252	-00277	-00014	-00038	-00023	+00102
3.0	+00315	-00270	-00031	-00020	-00038	+00104
3.1	+00376	-00251	-00056	-00003	-00052	+00102
3.2	+00424	-00221	-00086	+00007	-00060	+00091
3.3	+00454	-00183	-00119	+00012	-00060	+00076
3.4	+00472	-00142	-00154	+00009	-00058	+00061
3.5	+00480	-00097	-00189	-00005	-00053	+00051
3.6	+00478	-00052	-00220	-00029	-00042	+00047
3.7	+00465	-00007	-00249	-00062	-00027	+00047
3.8	+00444	+00033	-00270	-00101	-00008	+00053
3.9	+00416	+00068	-00278	-00141	+00012	+00065
4.0	+00387	+00095	-00269	-00174	+00031	+00080
4.1	+00357	+00113	-00247	-00190	+00043	+00088
4.2	+00306	+00122	-00218	-00185	+00049	+00089
4.3	+00254	+00116	-00187	-00174	+00039	+00087
4.4	+00206	+00095	-00154	-00151	+00026	+00079
4.5	+00162	+00053	-00139	-00120	+00018	+00086
4.6	+00123	+00013	-00124	-00090	+00009	+00088
4.7	+00091	-00004	-00096	-00070	-00002	+00067
4.8	+00061	-00001	-00055	-00048	-00003	+00028

Fourier coefficients for Run 26 field (cont.)

r model inches	B_3 gauss	B_6 gauss	B_9 gauss	B_{12} gauss	B_{15} gauss	B_{18} gauss
0.1	+00018	+00002	+00001	+00000	+00000	+00000
0.2	+00123	+00014	+00006	+00007	+00004	+00004
0.3	+00331	+00026	+00019	+00010	+00011	+00008
0.4	+00622	+00030	+00028	+00014	+00011	+00011
0.5	+00994	+00024	+00037	+00020	+00012	+00014
0.6	+01405	+00020	+00035	+00027	+00013	+00015
0.7	+01812	+00017	+00030	+00028	+00016	+00015
0.8	+02190	+00040	+00034	+00026	+00014	+00014
0.9	+02548	+00067	+00041	+00018	+00014	+00014
1.0	+02883	+00086	+00052	+00016	+00015	+00014
1.1	+03194	+00100	+00077	+00019	+00013	+00014
1.2	+03484	+00105	+00111	+00025	+00013	+00016
1.3	+03755	+00097	+00157	+00034	+00011	+00018
1.4	+04004	+00080	+00207	+00036	+00013	+00017
1.5	+04235	+00070	+00259	+00032	+00020	+00014
1.6	+04444	+00082	+00309	+00027	+00025	+00016
1.7	+04622	+00121	+00359	+00023	+00033	+00018
1.8	+04767	+00187	+00411	+00018	+00044	+00015
1.9	+04885	+00272	+00460	+00017	+00056	+00010
2.0	+04985	+00373	+00505	+00036	+00068	+00012
2.1	+05075	+00477	+00544	+00067	+00082	+00019
2.2	+05151	+00583	+00572	+00104	+00094	+00025
2.3	+05211	+00687	+00592	+00143	+00100	+00033
2.4	+05260	+00792	+00605	+00184	+00101	+00046
2.5	+05302	+00905	+00609	+00225	+00093	+00060
2.6	+05334	+01015	+00600	+00263	+00083	+00073
2.7	+05350	+01115	+00578	+00299	+00070	+00085
2.8	+05350	+01207	+00547	+00337	+00057	+00096
2.9	+05344	+01293	+00509	+00374	+00041	+00104
3.0	+05339	+01381	+00465	+00415	+00036	+00111
3.1	+05333	+01464	+00416	+00452	+00056	+00114
3.2	+05323	+01543	+00363	+00478	+00087	+00109
3.3	+05302	+01617	+00303	+00490	+00120	+00097
3.4	+05275	+01686	+00240	+00493	+00155	+00084
3.5	+05245	+01751	+00183	+00490	+00189	+00073
3.6	+05207	+01805	+00139	+00481	+00222	+00063
3.7	+05151	+01845	+00117	+00465	+00257	+00054
3.8	+05074	+01866	+00122	+00445	+00289	+00054
3.9	+04963	+01866	+00148	+00421	+00312	+00067
4.0	+04799	+01843	+00183	+00398	+00320	+00085
4.1	+04553	+01789	+00212	+00374	+00312	+00098
4.2	+04197	+01680	+00218	+00330	+00286	+00102
4.3	+03731	+01516	+00213	+00279	+00255	+00095
4.4	+03182	+01318	+00202	+00227	+00216	+00084
4.5	+02605	+01103	+00192	+00170	+00184	+00088
4.6	+02061	+00889	+00170	+00124	+00153	+00089
4.7	+01595	+00691	+00136	+00091	+00119	+00067
4.8	+01232	+00520	+00091	+00061	+00074	+00028

Fourier amplitudes as functions of radius Run 26

$$B_i(r) = \left(H_i^2(r) + G_i^2(r)\right)^{1/2}$$

$$B(r,0) = B_0(r) + \sum_{j=1} B_{3j}(r) \cos(jN\theta - \delta_{3j}(r))$$

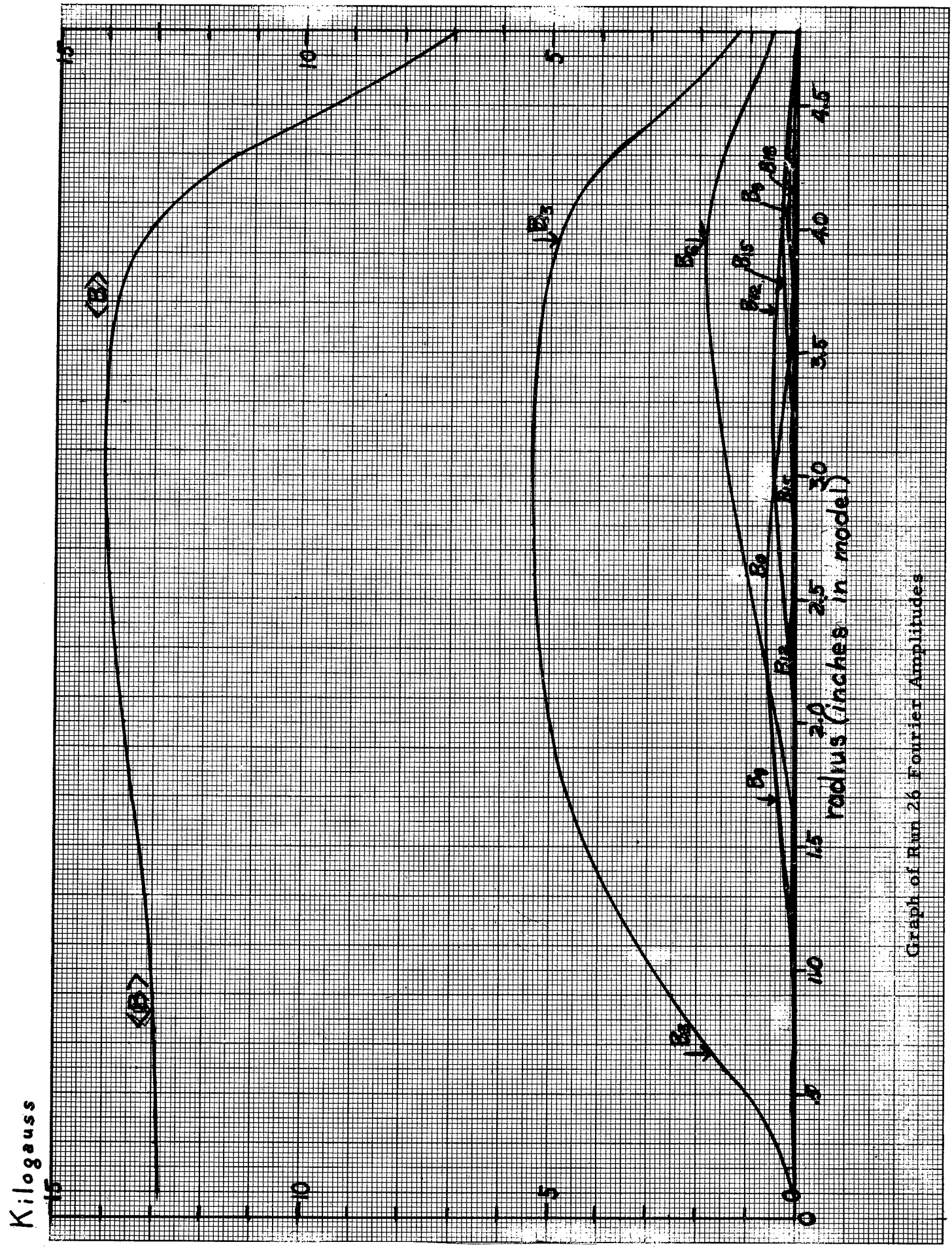

Graph of Run 26 Fourier Amplitudes

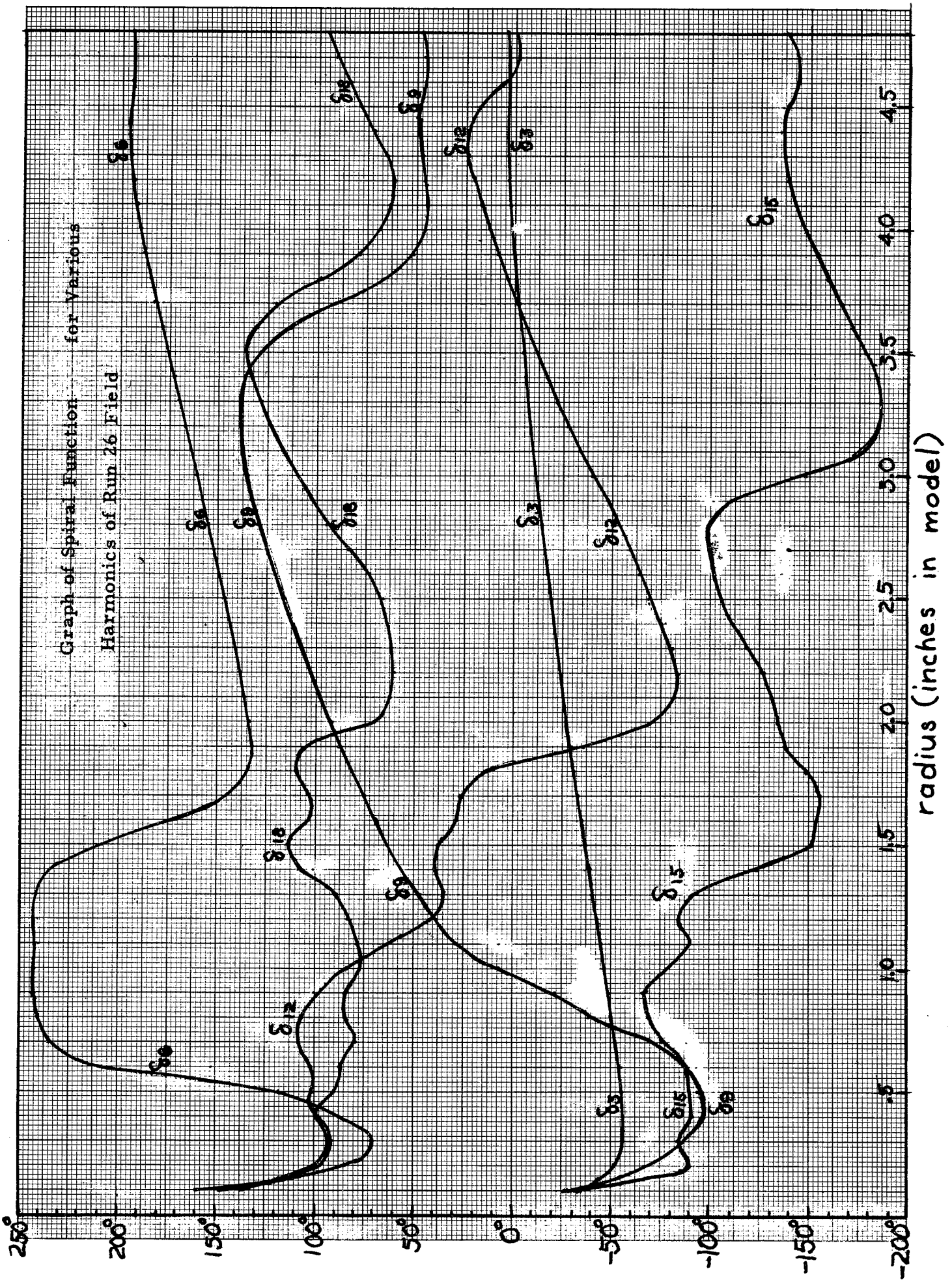
Graph of Spiral Function for Various
Harmonics of Run 26 Field
radius (inches in model)
250°
200°
150°
100°
50°
0°
-50°
-100°
-150°
-200°
.5
1.0
1.5
2.0
2.5
3.0
3.5
4.0
4.5